Biophysical Chemistry 172 (2013) 18–25

Contents lists available at SciVerse ScienceDirect

Biophysical Chemistry

journal homepage: http://www.elsevier.com/locate/biophyschem

NMR investigation on the DNA binding and B–Z transition pathway of the Zα domain of human ADAR1

Yeon-Mi Lee, Hee-Eun Kim, Eun-Hae Lee, Yeo-Jin Seo, Ae-Ree Lee, Joon-Hwa Lee *

Department of Chemistry and RINS, Gyeongsang National University, Jinju, Gyeongnam 660-701, Republic of Korea

HIGHLIGHTS

- Zα binds to CG-rich DNA segment maintaining B-DNA via a unique conformation.
- Zα significantly destabilizes A·T base pairs outside 8-bp CG-rich region.
- Four $Z\alpha_{ADAR1}$ protein monomers initially interact with the 8-bp DNA sequence, even though this segment contains A·T base pairs.

GRAPHICAL ABSTRACT

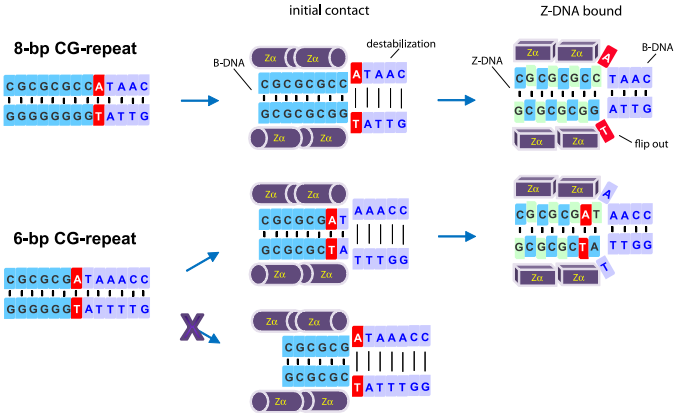

ARTICLE INFO

Article history:
Received 22 October 2012
Received in revised form 22 November 2012
Accepted 8 December 2012
Available online 21 December 2012

Keywords:
NMR
Z-DNA
DNA–protein interaction
Hydrogen exchange
Z-DNA binding protein

ABSTRACT

Human ADAR1, which has two left-handed Z-DNA binding domains, preferentially binds Z-DNA rather than B-DNA with a high binding affinity. Z-DNA can be induced in long genomic DNA by Z-DNA binding proteins through the formation of two B–Z junctions with the extrusion of one base pair from each junction. We performed NMR experiments on complexes of $Z\alpha_{ADAR1}$ with three DNA duplexes at a variety of protein-to-DNA molar ratios. This study confirmed that the $Z\alpha_{ADAR1}$ first binds to an 8-bp CG-rich DNA segment via a unique conformation during B–Z transition and the neighboring AT-rich region becomes destabilized. We also found that, when DNA duplexes have only 6-bp CG-rich segment, the interaction with $Z\alpha_{ADAR1}$ did not affect the thermal stabilities of the 6-bp CG-rich segment as well as the neighboring two A·T base pairs. These results indicate that four $Z\alpha_{ADAR1}$ proteins interact with the 8-bp DNA sequence containing a 6-bp CG-repeat segment as well as a dinucleotide step, even though the dinucleotid step contains A·T base pairs. Thus this study suggests that the length of the CG-rich region is more important than the specific DNA sequence for determining which base-pair is extruded from the B–Z junction structure. This study also found that the $Z\alpha_{ADAR1}$ in complex with a 11-bp DNA duplex exhibits a Z-DNA-bound conformation

Abbreviations: 1D, One dimensional; bp, Base-paired; P/N ratio, Protein-to-DNA molar ratio; ADAR1, Double-stranded RNA deaminase I; $Z\alpha_{ADAR1}$, Zα domain of human ADAR1.

* Corresponding author. Tel.: +82 55 772 1490; fax: +82 55 772 1489.
E-mail address: joonhwa@gnu.ac.kr (J.-H. Lee).

0301-4622/$ – see front matter
http://dx.doi.org/10.1016/j.bpc.2012.12.002

distinct from that of free $Z\alpha_{ADAR1}$ and the initial contact conformations of $Z\alpha_{ADAR1}$ complexed with 13-bp DNA duplexes.

1. Introduction

Under high-salt conditions, polymers of alternating $d(CG)_n$ sequences form the left-handed Z-DNA duplex, which is a higher energy conformation than B-DNA duplex [1,2]. Z-DNA is stabilized by complex formation with Z-DNA-binding proteins such as double-stranded RNA deaminase I (ADAR1), DNA-dependent activator of IFN regulatory factor, and poxvirus E3L protein [3–7]. Human ADAR1 has two Z-DNA binding domains at its N-terminus, Zα and Zβ, and preferentially binds to Z-DNA rather than B-DNA with high binding affinity [8–11]. The crystal structure of the Zα domain of human ADAR1 ($Z\alpha_{ADAR1}$) complexed to Z-DNA revealed that two Zα domains bind to each strand of the double-stranded Z-DNA with two-fold symmetry with respect to the DNA helical axis [3]. NMR studies of the $d(CGCGCG)_2$ segment (referred to as CG6) in complex with $Z\alpha_{ADAR1}$ suggested an active B–Z transition mechanism in which the $Z\alpha_{ADAR1}$ protein first binds to B-DNA and then converts it to left-handed Z-DNA, a conformation that is subsequently stabilized by the binding of a second $Z\alpha_{ADAR1}$ molecule [12].

An X-ray structural study of a 15 base-paired (15-bp) DNA duplex complexed with $Z\alpha_{ADAR1}$ showed that Z-DNA is produced with the help of $Z\alpha_{ADAR1}$ through the formation of a B–Z junction structure in which the DNA helices are stabilized at one end in the Z-conformation by $Z\alpha_{ADAR1}$ proteins while the other end remains as B-DNA [13]. This study also found that the B–Z junction structure is stabilized by continuous base stacking and the extrusion of one base pair at the junction [13]. Recently, NMR studies of a 13-bp DNA in complex with $Z\alpha_{ADAR1}$ have suggested a three-step mechanism of B–Z junction formation in which (*i*) $Z\alpha_{ADAR1}$ first binds to the CG-rich DNA segment maintaining B-DNA via a unique conformation, (*ii*) the neighboring AT-rich region then becomes destabilized and the CG-rich segment is converted to Z-DNA, and finally (*iii*) the B–Z junction is formed by base pairing of the AT-rich region [14]. Although this study clearly explained how Z-DNA can be produced in long genomic DNA by Z-DNA binding proteins, more experimental evidence is required to establish this as the generalized mechanism of B–Z junction formation.

We have conducted NMR studies on a 13-bp DNA duplex (referred to as bzDNA13b) and an 11-bp DNA duplex (referred to as bzDNA11), which form complexes with $Z\alpha_{ADAR1}$ in multiple protein-to-DNA molar ratios (P/N ratios). These results were compared to those from a previous study that used another 13-bp DNA duplex (referred to as bzDNA13a) [14]. We investigated the hydrogen exchange process of the imino protons of the three DNA duplexes in the complexes at various P/N ratios. The chemical shift perturbations in the amide backbone of $Z\alpha_{ADAR1}$ were also studied as a function of the P/N ratios. This study reveals key features of the binding interfaces of the DNA duplexes with $Z\alpha_{ADAR1}$ in the complex and provides information about the molecular mechanism of B–Z junction formation.

2. Materials and methods

2.1. Sample preparation

The bzDNA13a duplex, d[CGCGCGCCATAAC]/d[GTTATGGCGCGCG] (Fig. 1A), has the same DNA sequence as bzDNA13, which has been previously fully studied by NMR spectroscopy [14]. The bzDNA13b duplex, d[CGCGCGATAAACC]/d[GGTTTATCGCGCG], has a 6-bp CG-repeat segment in region I but has a 7-bp AT-rich region II (Fig. 1A). In the bzDNA11 duplex, d[CGCGCGATAAC]/d[GTTATCGCGCG], the sequence of region I is the same as in bzDNA13b but the base-pair pattern in region I is the same with bzDNA13a (Fig. 1A). The DNA oligomers were purchased from M-biotech Inc. (Seoul, Korea) and desalted using a Sephadex G-25 gel filtration column. The DNA duplexes were prepared by dissolving two DNA strands at a 1:1 stoichiometric ratio in a 90% H_2O/10% D_2O NMR buffer containing 10 mM sodium phosphate (pH 8.0) and 100 mM NaCl. To produce ^{15}N-labeled $Z\alpha_{ADAR1}$, BL21(DE3) bacteria expressing $Z\alpha_{ADAR1}$ were grown in M9 medium containing 1 g/L $^{15}NH_4Cl$. The expression and purification of ^{15}N-labeled $Z\alpha_{ADAR1}$ has been described in

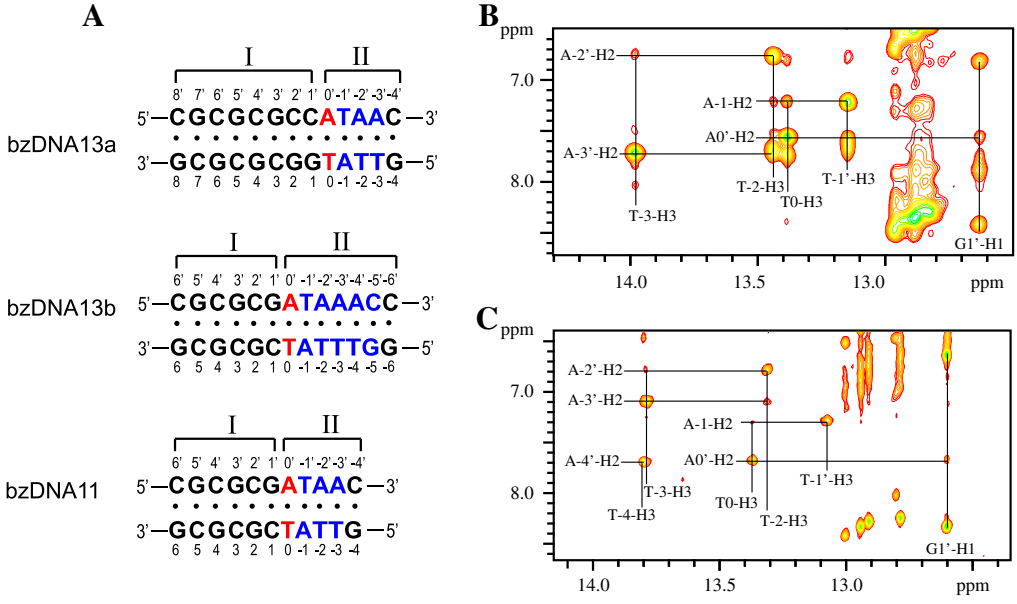

Fig. 1. (A) Sequence contexts of the 13-bp (bzDNA13a and bzDNA13b) and 11-bp (bzDNA11) DNA duplexes. Expanded NOESY (250 ms mixing time) contour plots of the (B) bzDNA13a at 5 °C and (C) bzDNA13b duplexes at 35 °C in 90% H_2O/10% D_2O NMR buffer. Solid lines indicate sequential NOE connectivities between the G/T imino and the A-H2/C-NH_2 protons.

a previous report [13]. The protein concentration was measured spectroscopically using an extinction coefficient of 6970 M^{-1} cm^{-1} at 280 nm.

2.2. NMR experiments

All experiments were performed on an Agilent 700 MHz NMR (GNU, Jinju) or Varian 900 MHz NMR spectrometer (KIST, Seoul) equipped with a triple resonance probe. All ^{1}H and ^{15}N NMR spectra were obtained using DNA–protein complex samples that were prepared by the addition of ^{15}N-labeled $Z\alpha_{ADAR1}$ to 0.2 mM DNA samples in NMR buffer at the indicated P/N ratio. One dimensional (1D) NMR data were processed with either the VNMRJ 3.2 (Agilent, Santa Clara) or FELIX2004 (Accelrys, San Diego) software, while the 2D data were processed with the NMRPipe software [15] and analyzed using the Sparky software [16]. External 2-2-dimethyl-2-silapentane-5-sulfonate was used for the ^{1}H and ^{15}N references.

The average chemical shift differences of the amide proton and nitrogen resonances between free $Z\alpha_{ADAR1}$ and $Z\alpha_{ADAR1}$ in complex with bzDNA11, bzDNA13a, or bzDNA13b were calculated using Eq. (1):

$$\Delta\delta_{avg} = \sqrt{(\Delta\delta_H)^2 + (\Delta\delta_N/5.88)^2} \quad (1)$$

where $\Delta\delta_H$ and $\Delta\delta_N$ are the chemical shift differences of the amide proton and nitrogen resonances, respectively.

The apparent longitudinal relaxation rate constants ($R_{1a} = 1/T_{1a}$) of the imino protons in the free DNA duplexes and the DNA–$Z\alpha_{ADAR1}$ complexes were determined by semi-selective inversion recovery 1D NMR experiments. The apparent relaxation rate constant of water (R_{1w}) was determined by a selective inversion recovery experiment, using a DANTE sequence for selective water inversion [17,18]. The hydrogen exchange rate constants (k_{ex}) of the imino protons were determined by a water magnetization transfer method, where a selective 180° pulse for water was applied, followed by a variable delay, and then a 3-9-19 acquisition pulse was used to suppress the water signal [17,18]. The intensities of imino protons were affected by exchanging with selectively inverted water signal and depends on their exchange rate constants. The intensities of each imino proton were measured with 20 different delay times. The k_{ex} for the imino protons were determined by fitting the data into Eq. (2):

$$\frac{I_0 - I(t)}{I_0} = 2\frac{k_{ex}}{(R_{1w} - R_{1a})}\left(e^{-R_{1a}t} - e^{-R_{1w}t}\right) \quad (2)$$

where I_0 and $I(t)$ are the intensities of the imino protons in the water magnetization transfer experiments at times zero and t, respectively, and R_{1a} and R_{1w} are the apparent longitudinal relaxation rate constants for the imino proton and water, respectively.

3. Results and discussion

3.1. Titration of $Z\alpha_{ADAR1}$ to bzDNA13b

The bzDNA13a duplex used in this study has the same DNA sequence as bzDNA13, which has been previously fully studied by NMR spectroscopy [14]. The bzDNA13b duplex has only six G·C base pairs in region I but has a 2-bp insertion (one A·T and one G·C base pair) in region II. 2D NOESY spectra were used to assign the imino proton resonances of the bzDNA13a and bzDNA13b duplexes (see Fig. 1). Interestingly, the T-2 imino proton resonance of the bzDNA13b duplex exhibits up-field chemical shift change compared to the bzDNA13a duplex, evident by the sequential NOE cross-peaks between the T-imino and A-H2 protons (Fig. 1B and C). Fig. 2A and B show the 1D imino proton spectra of the bzDNA13a–$Z\alpha_{ADAR1}$ and bzDNA13b–$Z\alpha_{ADAR1}$ complexes at various P/N ratios. As the P/N ratio is increased, the peak intensities for the T-2 and T-3 imino protons in the bzDNA13a duplexes significantly decreased until they completely disappeared at P/N ratio = 1.0 (Fig. 2A), as mentioned in the previous study [14]. This result demonstrates that the T-2·A-2′ and T-3·A-3′ base pairs of the bzDNA13a duplex are significantly destabilized upon binding to the $Z\alpha_{ADAR1}$ protein. Similarly, in the bzDNA13b duplex, a decrease in peak intensities for the T-4 and G-5 imino protons was observed with an increasing P/N ratio (Fig. 2B).

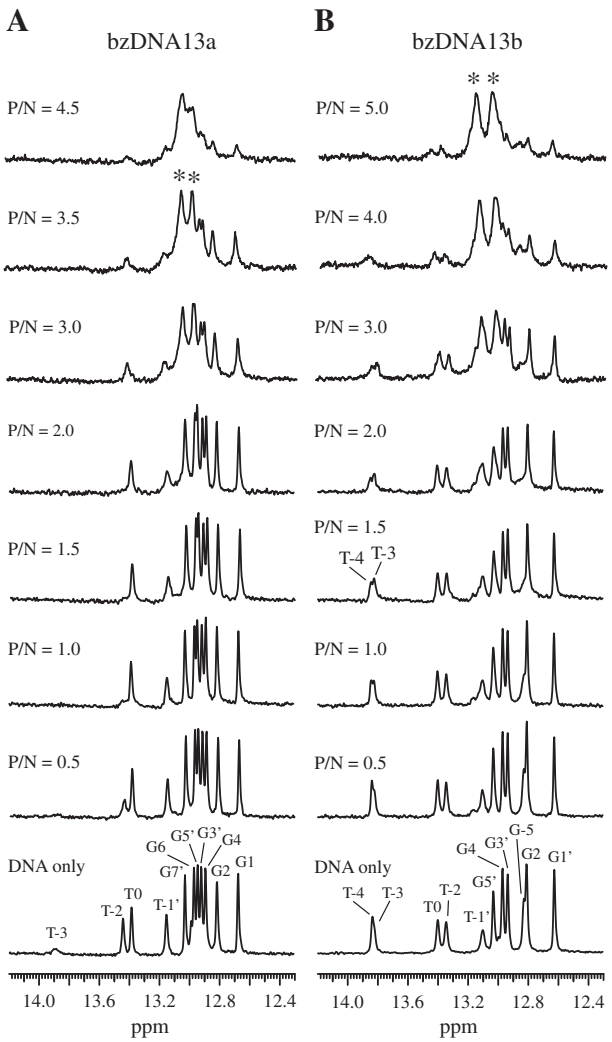

Fig. 2. 1D imino proton spectra of the (A) bzDNA13a [14] and (B) bzDNA13b duplexes at 35 °C upon titration with $Z\alpha_{ADAR1}$. The P/N ratios are shown to the left of each spectrum. The asterisk symbols indicate the G-imino proton resonances of Z-form DNA duplexes.

The line-broadening effects in the 1D imino proton spectra induced by $Z\alpha_{ADAR1}$ binding were observed more clearly in both DNA duplexes at P/N ratio > 1 (Fig. 2A and B). Surprisingly, when the P/N ratio ≥ 3.0, new imino proton resonances (denoted as asterisk) can be observed in the both bzDNA13a and bzDNA13b duplexes (Fig. 2A and B). The pattern of these two imino proton resonances is very similar to that of the Z-form helix of $d(CGCGCG)_2$ induced by $Z\alpha_{ADAR1}$ [12]. In addition, at P/N ratio = 4.5, the B–Z transition of the bzDNA13a upon addition of $Z\alpha_{ADAR1}$ was confirmed by ^{31}P NMR spectra in the previous study [14]. Thus these new resonances (denoted as asterisk) in the imino proton spectra are indicative of left-handed Z-form helix generation in the DNA duplexes induced by $Z\alpha_{ADAR1}$. The severe line-broadening of the imino proton resonances of the Z-form helix is indicative of the larger molecular size of DNA–$Z\alpha_{ADAR1}$ complexes compared to the free DNA duplexes.

3.2. Exchange rate constants of imino protons of bzDNA13b complexed with $Z\alpha_{ADAR1}$

The k_{ex} of the imino protons in free bzDNA13b were determined at 35 °C by the water magnetization transfer method [17,18]. Rapidly exchanging imino protons, such as T-4 and G-5, show very weak peaks at a delay time of 100 ms, whereas the resonance of the G1 imino proton, which is the slowest exchanging imino proton, remains basically unchanged up to 100 ms (Fig. 3A, left). The k_{ex} values of the imino protons of the bzDNA13b duplex were determined by curve fitting to Eq. (2). The G imino protons in the CG-repeat region (region I) have slightly larger k_{ex} values compared to those in free bzDNA13a in the previous study [14]. These exchange data indicate that at 35 °C, the base pairs in region I of bzDNA13b are less stable than those of the bzDNA13a. However, the T imino protons in the AT-rich region (region II) have k_{ex} values ranging from 2.7 to 7.3 s^{-1}, which is significantly smaller than that of free bzDNA13a reported in the previous study [14], suggesting higher base pair stabilities of region II in the bzDNA13b compared to bzDNA13a at 35 °C.

To examine the interacting region of bzDNA13b with $Z\alpha_{ADAR1}$, the k_{ex} of the imino protons in the bzDNA13b–$Z\alpha_{ADAR1}$ complexes at various P/N ratios were determined at 35 °C and compared with the k_{ex} of the imino protons in free bzDNA13b (Fig. 3). In the bzDNA13b–$Z\alpha_{ADAR1}$ complex at P/N = 0.8, the T-4 and G-5 imino protons show negative peaks at a delay time of 100 ms (Fig. 3A). These results mean that, in contrast to free bzDNA13b, the more than 50% of T-4 and G-5 imino protons exchanged with magnetically inverted solvent water during delay time of 100 ms. The k_{ex} values of the T-4 (27.4 s^{-1}) and G-5 (35.9 s^{-1}) imino protons in the bzDNA13b–$Z\alpha_{ADAR1}$ complex at P/N = 0.8 are 3-fold larger than those of free bzDNA13b (Fig. 4). The T-2 and T-3 imino protons also show much larger differences in peak intensities as a function of delay time after water inversion compared to free bzDNA13b (Fig. 3B). This leads to 2-fold larger k_{ex} values of the T-2 (5.4 s^{-1}) and T-3 (6.9 s^{-1}) imino protons in the bzDNA13b–$Z\alpha_{ADAR1}$ complex at P/N = 0.8 than those of free bzDNA13b (Fig. 4). These imino protons undergo a more rapid exchange with solvent water as the P/N ratio increases (Fig. 4), suggesting that the interaction of bzDNA13b with $Z\alpha_{ADAR1}$ significantly destabilizes

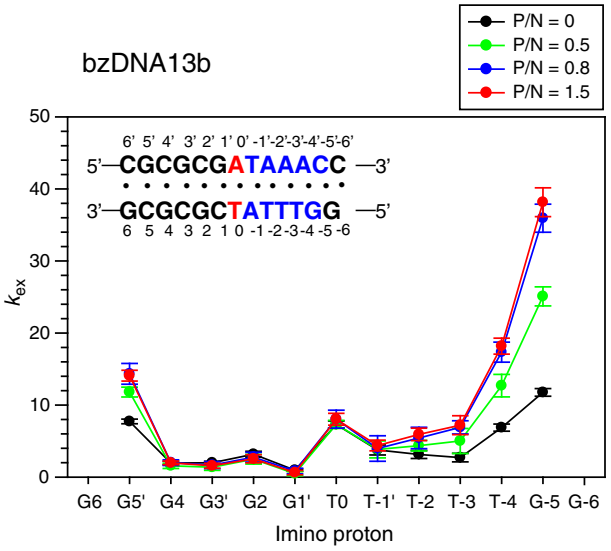

Fig. 4. The hydrogen exchange rate constants of the imino protons of free bzDNA13b (black) and the bzDNA13b–$Z\alpha_{ADAR1}$ complexes (P/N = 0.5, green; 0.8, blue; 1.5, red) at 35 °C.

four base pairs (−2 to −5 positions) in region II. The same phenomenon was also observed in the four A·T base pairs (0 to −3 positions) in region II of bzDNA13a in the previous report [14]. Similarly, the k_{ex} value for the G5′ imino proton significantly increased to 38.2 s^{-1} as the P/N ratio increased (Fig. 4). However, like bzDNA13a in previous study [14], no increase in exchange was observed for the G imino protons in region I except the G5′ imino proton (Fig. 3B), suggesting that the bzDNA13b–$Z\alpha_{ADAR1}$ interaction had little effect on the k_{ex} values of the G·C base pairs in region I.

In the previous study, in the bzDNA13a–$Z\alpha_{ADAR1}$ complex at P/N = 0.9, the k_{ex} values of the T-1′ and T0 imino protons are 6- and 5-fold larger than those of free bzDNA13a, respectively [14]. However, in the bzDNA13b–$Z\alpha_{ADAR1}$ complex at P/N = 0.8, the T-1′ and T0 imino

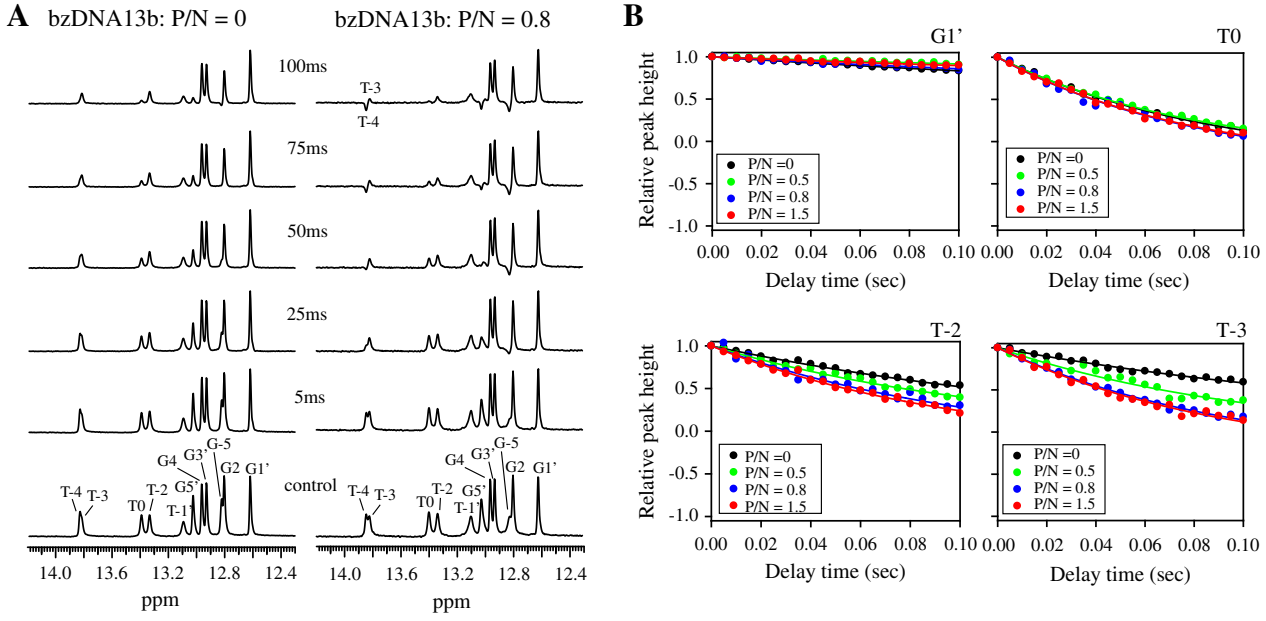

Fig. 3. (A) 1D imino proton spectra of the water magnetization transfer experiments for free bzDNA13b (left) and the bzDNA13b–$Z\alpha_{ADAR1}$ complex at P/N = 0.8 (right) at 35 °C. The delay times after water inversion are shown between the two spectra. (B) Relative peak height [$I(t)/I_0$] in the water magnetization transfer spectra for the G1′, T0, T2, and T3 imino protons of free bzDNA13b (black) and the bzDNA13b–$Z\alpha_{ADAR1}$ complexes (P/N = 0.5, green; 0.8, blue; 1.5, red) as a function of delay time. Solid lines indicate the best fitting data using Eq. (2).

protons show no differences in peak intensities as a function of delay time compared to free bzDNA13b (Fig. 3B). Thus, in the bzDNA13b–$Z\alpha_{ADAR1}$ complex at P/N = 0.8, the T-1′ (4.0 s^{-1}) and T0 (8.0 s^{-1}) imino protons have k_{ex} values similar to those of free bzDNA13b (Fig. 4). The exchange constants remained unchanged for the T–1′ and T0 imino protons in the bzDNA13b–$Z\alpha_{ADAR1}$ complex at various P/N ratios (Fig. 4). These results indicated that unlike bzDNA13a, the interaction of bzDNA13b with $Z\alpha_{ADAR1}$ did not affect the thermal stabilities of the A-1′·T-1′ and T0·A0′ base pairs.

3.3. Chemical shift perturbation of $Z\alpha_{ADAR1}$ upon binding to bzDNA13b

A superimposition of the $^1H/^{15}N$-HSQC resonances for some amide residues in free $Z\alpha_{ADAR1}$, $Z\alpha_{ADAR1}$–CG6 (P/N = 2.0), $Z\alpha_{ADAR1}$–bzDNA13a (P/N = 0.5), and $Z\alpha_{ADAR1}$–bzDNA13b (P/N = 0.5 and 1.5) is shown in Fig. 5. The $^1H/^{15}N$-HSQC spectra of the $Z\alpha_{ADAR1}$–bzDNA13b complexes (P/N = 0.5 and 1.5) are completely different from that of the $Z\alpha_{ADAR1}$–CG6 complex (P/N = 2.0). Like bzDNA13a in the previous study [14], the residues of $Z\alpha_{ADAR1}$ underwent $\Delta\delta_{avg} < 0.15$ ppm upon binding to bzDNA13b when the P/N ratio < 1 (*data not shown*). Interestingly, in the $Z\alpha_{ADAR1}$–bzDNA13b complex (P/N = 0.5), most amide signals are located very close to those of the $Z\alpha_{ADAR1}$–bzDNA13a (P/N = 0.5) rather than to the free $Z\alpha_{ADAR1}$ and the $Z\alpha_{ADAR1}$–CG6 (P/N = 2.0) (Fig. 5). These $^1H/^{15}N$-HSQC spectra show that the $Z\alpha_{ADAR1}$ in complex with bzDNA13b at P/N ≤ 1 has a conformation similar to that of the $Z\alpha_{ADAR1}$–bzDNA13a complex (P/N ≤ 1), but this conformation is distinct from free $Z\alpha_{ADAR1}$ and $Z\alpha_{ADAR1}$ in complex with CG6 (Z-DNA).

At a P/N ratio = 1.5, the $Z\alpha_{ADAR1}$–bzDNA13b complex exhibits two E171 amide signals similar to bzDNA13a in the previous study [14]; one close to the free form signal and the other close to that for the $Z\alpha_{ADAR1}$–CG6 complex (Fig. 5B). Similar results were also observed in the amide signals for A180 (Fig. 5C) and G163 and G190 (Fig. 5D). Thus, we can summarize that: (*i*) when the P/N ≤ 1, the $Z\alpha_{ADAR1}$ interacts with bzDNA13a or bzDNA13b via a unique initial contact conformation and (*ii*) when the P/N ≥ 1.5, $Z\alpha_{ADAR1}$ exhibits properties of both the initial contact conformation and the Z-DNA-bound conformation.

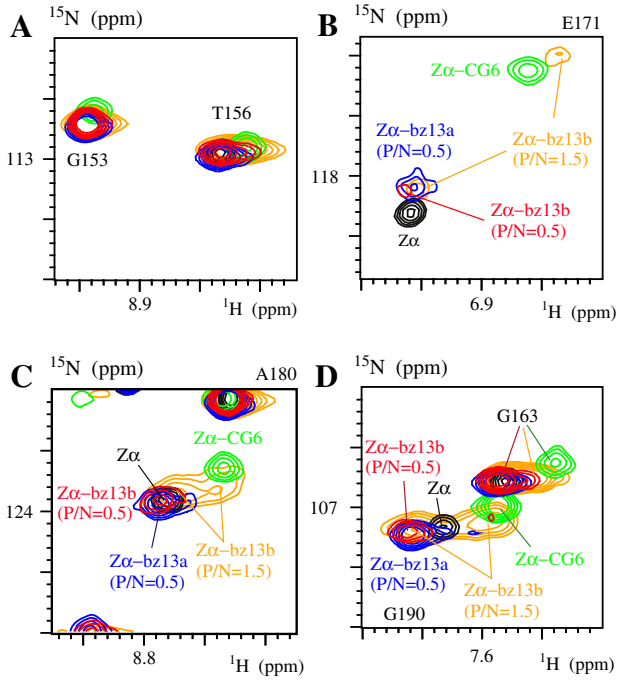

Fig. 5. Comparison of the $^1H/^{15}N$-HSQC peaks of (A) G153/T156, (B) E171, (C) A180, and (D) G163/G190 amide protons of $Z\alpha_{ADAR1}$ in the free (black) and in a complex with CG6 at P/N = 2.0 (green), bzDNA13a at P/N = 0.5 (blue), and bzDNA13b at P/N = 0.5 (red) and 1.5 (orange) at 35 °C.

3.4. NMR study on the $Z\alpha_{ADAR1}$–bzDNA11 complex

To clarify our observation, we performed NMR study on the bzDNA11 duplex (Fig. 1A), in which the sequence of region II is the same as in bzDNA13a but two G·C base pairs in region I have been removed like bzDNA13b. 2D NOESY spectra were used to assign the imino proton resonances of the bzDNA11 duplex (data not shown). Fig. 6A shows the 1D imino proton spectra of the bzDNA11–$Z\alpha_{ADAR1}$ complex at various P/N ratios. Similar to bzDNA13a, as the P/N ratio is increased, the peak intensities for the T-2 and T-3 imino protons in the bzDNA11 duplex significantly decreased until they completely disappeared at P/N ratio = 1.0 (Fig. 6A). These results demonstrate that the T-2·A-2′ and T-3·A-3′ base pairs of both duplexes are significantly destabilized upon binding to the $Z\alpha_{ADAR1}$ protein. At P/N ratio > 1, the line-broadening effects of the imino proton resonances induced by $Z\alpha_{ADAR1}$ binding were also observed clearly (Fig. 6A), which is indicative of the larger molecular size of bzDNA11–$Z\alpha_{ADAR1}$ complex compared to the free bzDNA11 duplex.

The k_{ex} of the imino protons in the free and bzDNA11 and bzDNA11–$Z\alpha_{ADAR1}$ complex at the P/N = 0.3 were determined at 35 °C (Fig. 6B). Like bzDNA13a in the previous study [14], the T-3 and T-2 imino protons of bzDNA11 show no peaks at a delay time of 75 ms (Fig. 6B, left), whereas the resonance of the G1 imino proton, which is the slowest exchanging imino proton, remains basically unchanged up to 100 ms (Fig. 6B, left). The T imino protons in the AT-rich region (region II) have k_{ex} from 4.5 to 50.0 s^{-1}, whereas, except for the terminal and C5·G5′ base pairs, the G imino protons in the CG-repeat region (region I) all have $k_{ex} < 2.0$ s^{-1}.

As expected from the bzDNA13a study [14], the T-3 and T-2 imino protons in the bzDNA11–$Z\alpha_{ADAR1}$ complex at P/N = 0.3 show much larger differences in peak intensities as a function of delay time after water inversion compared to free bzDNA11. Thus, the k_{ex} values of the T-3 (64.2 s^{-1}) and T-2 (14.9 s^{-1}) imino protons in the bzDNA11–$Z\alpha_{ADAR1}$ complex at P/N = 0.3 are slightly larger than those of free bzDNA11 (Fig. 6C). In addition, the G5′ imino proton in this complex has a k_{ex} value of 4.8 s^{-1}, which is larger than that of free bzDNA11 (3.7 s^{-1}) (Fig. 6C). Similar to bzDNA13a and bzDNA13b, no enhancement of exchange was observed for G imino protons in region I, except for the G5′ imino proton (Fig. 6C). The previous study reported that in the bzDNA13a–$Z\alpha_{ADAR1}$ complex at P/N = 0.3, the k_{ex} values of the T-1′ and T0 imino protons are 2.5-fold larger than those of free bzDNA13a [14]. However, in the bzDNA11–$Z\alpha_{ADAR1}$ complex at P/N = 0.3, the k_{ex} values of the T-1′ and T0 imino protons were found to be the same as that of free bzDNA11 (Fig. 6C), even though both DNA duplexes have the same DNA sequence in AT-rich region II. Instead, the similar phenomenon was observed in the bzDNA13b–$Z\alpha_{ADAR1}$ complexes (Fig. 4). This result suggests that in the DNA–$Z\alpha_{ADAR1}$ complexes, the k_{ex} values for the T0·A0′ and A-1·T-1′ base pairs are independent of AT-rich region II sequence but are influenced by the length of GC-rich region I.

A superimposition of the $^1H/^{15}N$-HSQC resonances for some amide residues in free $Z\alpha_{ADAR1}$, $Z\alpha_{ADAR1}$–CG6 (P/N = 2), $Z\alpha_{ADAR1}$–bzDNA13a (P/N = 0.5), and $Z\alpha_{ADAR1}$–bzDNA11 (P/N = 0.3) is shown in Fig. 6D. We observed that even at P/N = 0.3, the $^1H/^{15}N$-HSQC spectra of the $Z\alpha_{ADAR1}$–bzDNA11 complexes are completely different from that of the $Z\alpha_{ADAR1}$–bzDNA13a complex (P/N = 0.5). Some residues of $Z\alpha_{ADAR1}$ underwent $\Delta\delta_{avg} > 0.2$ ppm upon binding to bzDNA11 (*data not shown*). Interestingly, in contrast to bzDNA13a and bzDNA13b, in the $Z\alpha_{ADAR1}$–bzDNA11 complex (P/N = 0.3), the E171 amide signal is located closer to that of the $Z\alpha_{ADAR1}$–CG6 complex rather than free $Z\alpha_{ADAR1}$ (Fig. 6D). Similar results were also observed in the amide signals for L172 and A180 (Fig. 6D). The V175 residue shows no amide signal in the $Z\alpha_{ADAR1}$–bzDNA13a (P/N = 0.5), but in the $Z\alpha_{ADAR1}$–bzDNA11

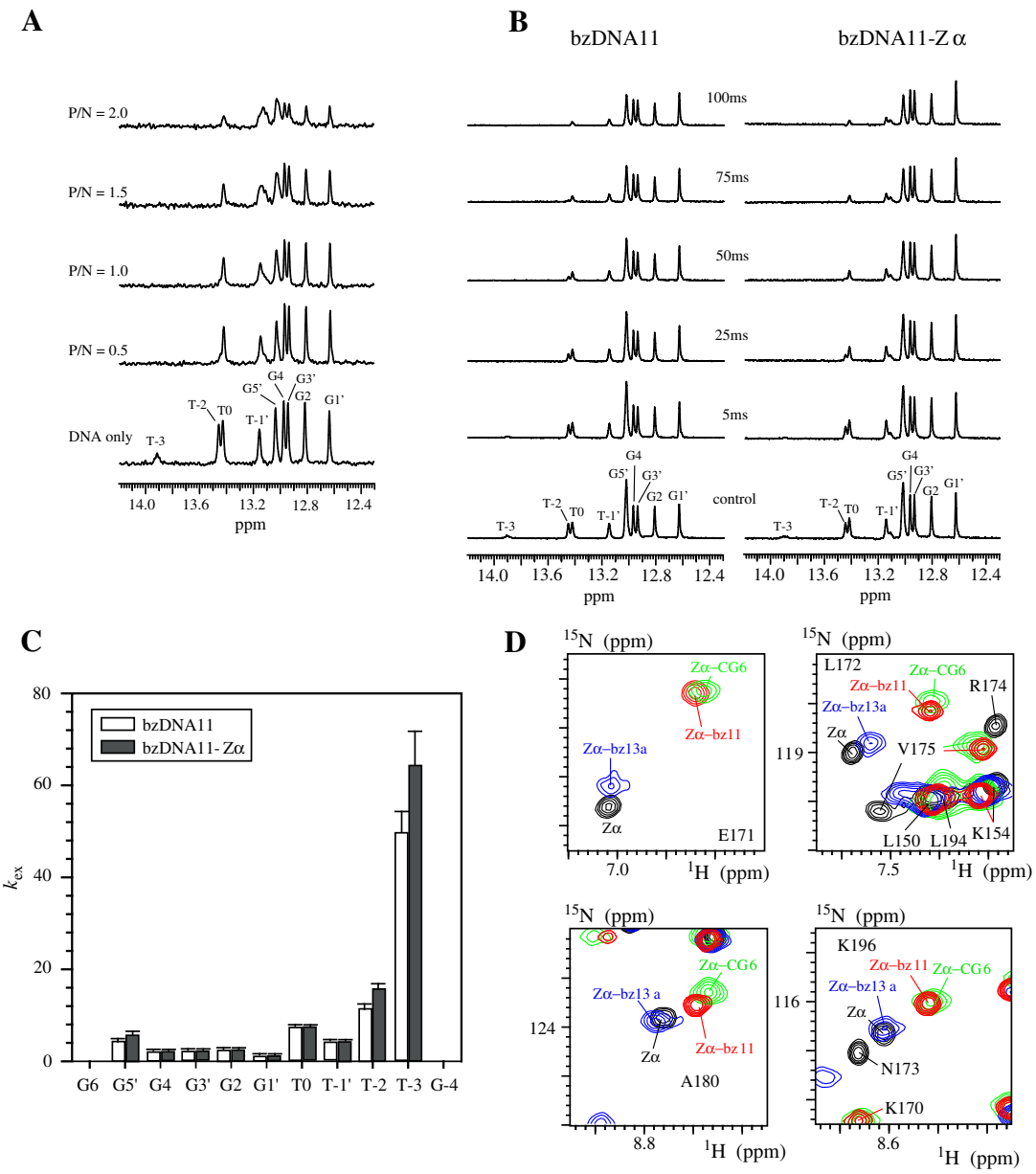

Fig. 6. (A) 1D imino proton spectra of the bzDNA11 duplex at 35 °C upon titration with $Z\alpha_{ADAR1}$. The P/N ratios are shown to the left of each spectrum. (B) 1D imino proton spectra of the water magnetization transfer experiments for free bzDNA11 (left) and the bzDNA11–$Z\alpha_{ADAR1}$ complex (P/N = 0.3) (right) at 35 °C. The delay times after water inversion are shown between the two spectra. (C) The hydrogen exchange rate constants of the imino protons of free bzDNA11 (open bar) and the bzDNA11–$Z\alpha_{ADAR1}$ complex (P/N = 0.3) (closed bar) at 35 °C. (D) Comparison of the $^{1}H/^{15}N$-HSQC peaks of E171, L172/V175, A180, and K196 amide protons of $Z\alpha_{ADAR1}$ in the free (black) and in a complex with CG6 at P/N = 2.0 (green), bzDNA13a at P/N = 0.5 (blue), and bzDNA11 at P/N = 0.3 (red) at 35 °C.

complex (P/N = 0.3), its amide resonance is observed near the corresponding signal of the $Z\alpha_{ADAR1}$–CG6 complex (Fig. 6D). These $^{1}H/^{15}N$-HSQC spectra show that the $Z\alpha_{ADAR1}$ in complex with bzDNA11 at P/N = 0.3 exhibits a Z-DNA-bound conformation distinct from that of free $Z\alpha_{ADAR1}$ and the initial contact conformations of $Z\alpha_{ADAR1}$ complexed with either bzDNA13a or bzDNA13b.

3.5. Implication for B–Z junction formation of DNA duplexes induced by $Z\alpha_{ADAR1}$

Polymers of alternating pyrimidine–purine nucleotides form left-handed Z-DNA helices in the presence of high-salt, negative super-coiling, or Z-DNA binding proteins [1–7]. The Zα domains of various Z-DNA binding proteins have a similar mechanism by which they bind to a 6-bp DNA segment, $d(CGCGCG)_2$. One Zα protein molecule binds to one strand of the duplex Z-DNA, while a second monomer binds to the opposite strand, yielding two-fold symmetry with respect to the DNA helical axis [3,4,6,7]. Z-DNA can also be induced in long genomic DNA sequences by Z-DNA binding proteins through the formation of two B–Z junctions with the extrusion of one base pair from each junction [13]. The B–Z junction formation of a 15-bp DNA duplex requires four molecules of the $Z\alpha_{ADAR1}$ protein; two molecules bind to one strand of the Z-DNA segment, while the other two molecules bind to the opposite strand [13]. Previous NMR studies of the bzDNA13a duplex in complex with $Z\alpha_{ADAR1}$ demonstrated that during $Z\alpha_{ADAR1}$-induced B–Z junction formation, the initial contact conformation possesses an intermediate structure (Fig. 7) [14]. In this conformation, the $Z\alpha_{ADAR1}$ protein displays unique backbone conformational changes distinct from its Z-DNA-bound conformation, but DNA duplex maintains the B-form helix (Fig. 7) [14].

The crystal structural study revealed that four molecules of the $Z\alpha_{ADAR1}$ proteins interact with the 8-bp DNA sequence including not only a 6-bp CG-repeat segment (3 to 8 position in bzDNA13a) but also GG/CC dinucleotide step (1 and 2 position in bzDNA13a) [13]. Recently, it was suggested that the length and sequence of this dinucleotide step is very important for the B–Z transition of the neighboring 6-bp CG-repeat segment [19]. Previous NMR study revealed that the $Z\alpha_{ADAR1}$ protein did not affect the exchange process of the G-imino protons in the CG-rich region I (1 to 6 position) of the bzDNA13a duplex in the initial contact conformation [14]. Instead, the $Z\alpha_{ADAR1}$ significantly destabilizes four A·T base pairs (−3 to 0 position) in AT-rich region II while physically interacting with CG-rich region II (Fig. 7) [14]. The instability of the AT-rich region II allows the CG-rich region I to convert easily to Z-DNA, just like in a CG-repeat DNA duplex [14]. Among these A·T base pairs, the T0·A0′ base pair displays base-pair extrusion in the final B–Z junction structure for continuous base stacking between the Z-form helix of the CG-rich region I and B-DNA of the AT-rich region II [13].

The $Z\alpha_{ADAR1}$ protein can induce the B–Z junction formation of the bzDNA13b duplex, which has only a 6-bp CG-repeat segment (1 to 6 position in bzDNA13b) in region I but has a 7-bp AT-rich region II (−6 and 0 position in bzDNA13b) (Fig. 1A). Interestingly, in the initail contact conformation, $Z\alpha_{ADAR1}$ interacts with bzDNA13b via the same backbone conformation as observed with bzDNA13a (Fig. 5). In contrast to bzDNA13a, the k_{ex} values for the T0·A0′ and A-1·T-1′ base pairs in the bzDNA13b duplex, did not increase although other A·T base pairs (−4 to −2 position) in AT-rich region II were significantly destabilized by the addition of $Z\alpha_{ADAR1}$ (Fig. 4). This result suggests that in the inital contact formation, the $Z\alpha_{ADAR1}$ molecules interacts with the 8-bp DNA sequence, including 6-bp CG-repeat segment and two A·T base pairs (Fig. 7). In the final $Z\alpha_{ADAR1}$-induced B–Z junction structure of bzDNA13b, to maintain continuous base stacking between B-DNA and Z-DNA, the bases of the T-2·A-2′ base pair, instead of the T0·A0′ base pair mentioned in bzDNA13a or 15-bp DNA duplexes in previous studies [13,14], are extruded (Fig. 7). Similarly, in the 11-bp bzDNA11 duplex, which contains a 6-bp CG-repeat segment like bzDNA13b but has only a 5-bp AT-rich region II, the k_{ex} values for the T0·A0′ and A-1·T-1′ base pairs did not increase upon the addition of $Z\alpha_{ADAR1}$ (Fig. 6C). However, in bzDNA11, the unstable AT-rich region II spans only 3 base pairs and therefore cannot strongly interfere with B–Z transition of the 8-bp region I (Fig. 7). Thus, the $Z\alpha_{ADAR1}$ protein adopt a backbone conformation that is significantly distinct from the ininitial contact conformation but is similar to that in the $Z\alpha_{ADAR1}$–Z–DNA complex (Fig. 6D).

These results indicate that four $Z\alpha_{ADAR1}$ protein monomers initially interact with the 8-bp DNA sequence containing a 6-bp CG-repeat segment as well as a dinucleotide step maintaining B-form helix via a unique conformation, even though the dinucleotid step contains A·T base pairs. Thus, we concluded that when $Z\alpha_{ADAR1}$ proteins induce the CG-repeat segments in a long DNA seqgence, the length of CG-rich region is more important than the DNA sequence to decide which base pair is extruded from the B–Z junction structure.

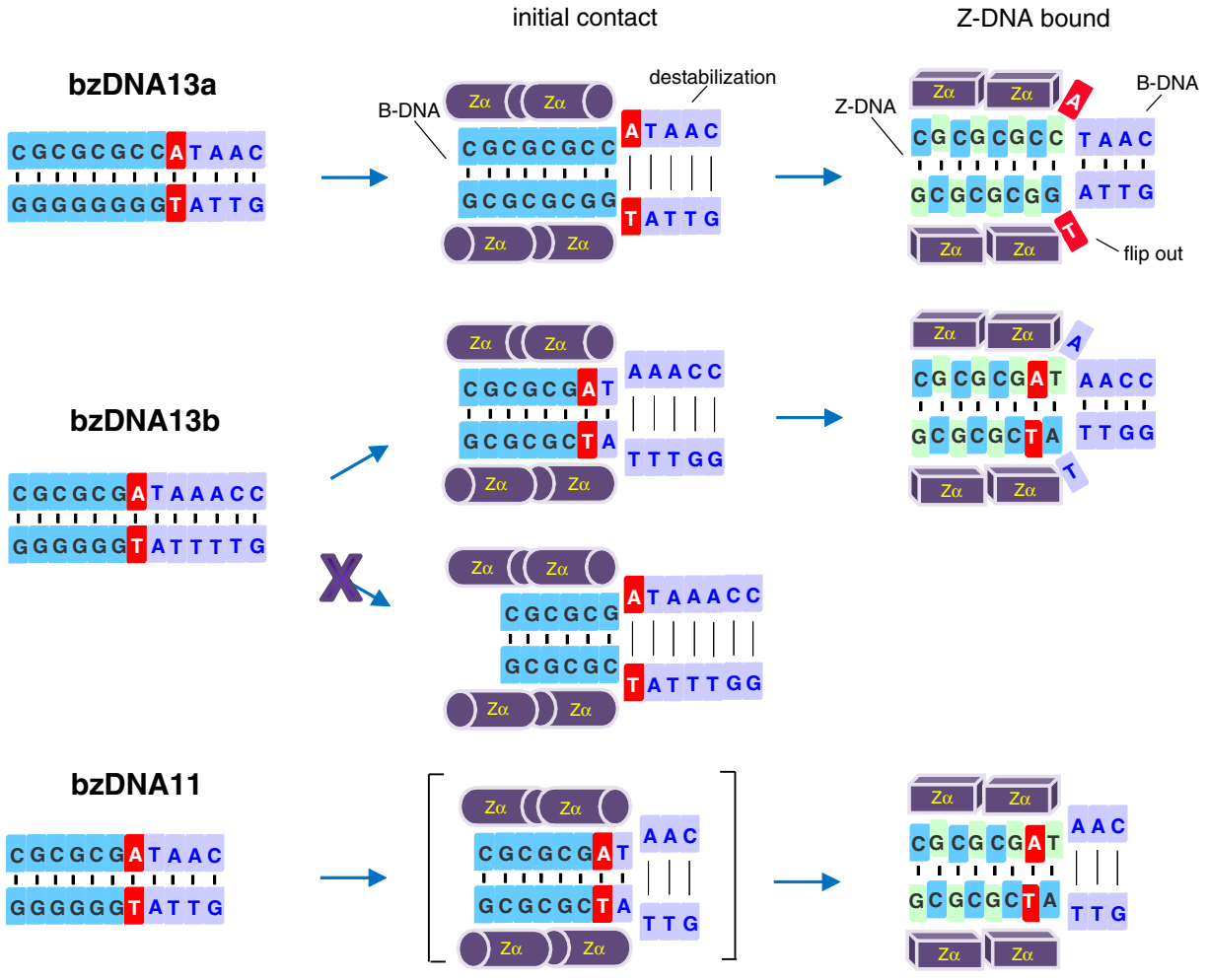

Fig. 7. Summary for suggested mechanism of B–Z junction formation of bzDNA13a, bzDNA13b, and bzDNA11 duplexes induced by four molecules of $Z\alpha_{ADAR1}$.

4. Conclusion

Human ADAR1, which has two left-handed Z-DNA binding domains, preferentially binds Z-DNA rather than B-DNA with a high binding affinity. Z-DNA can be induced in long genomic DNA by Z-DNA binding proteins through the formation of two B–Z junctions with the extrusion of one base pair from each junction. We performed NMR experiments on complexes of $Z\alpha_{ADAR1}$ with three DNA duplexes at a variety of protein-to-DNA molar ratios. This study confirmed that the $Z\alpha_{ADAR1}$ first binds to an 8-bp CG-rich DNA segment via a unique conformation during B–Z transition and the neighboring AT-rich region becomes destabilized. We also found that, when DNA duplexes have only 6-bp CG-rich segment, the interaction with $Z\alpha_{ADAR1}$ did not affect the thermal stabilities of the 6-bp CG-rich segment as well as the neighboring two A·T base pairs. These results indicate that four $Z\alpha_{ADAR1}$ proteins interact with the 8-bp DNA sequence containing a 6-bp CG-repeat segment as well as a dinucleotide step, even though the dinucleotid step contains A·T base pairs. Thus this study suggests that the length of the CG-rich region is more important than the specific DNA sequence for determining which base-pair is extruded from the B–Z junction structure. This study also found that the $Z\alpha_{ADAR1}$ in complex with a 11-bp DNA duplex exhibits a Z-DNA-bound conformation distinct from that of free $Z\alpha_{ADAR1}$ and the initial contact conformations of $Z\alpha_{ADAR1}$ complexed with 13-bp DNA duplexes. This study strongly supports the following mechanism for B–Z junction formation in long genomic DNA: (*i*) $Z\alpha_{ADAR1}$ first binds to CG-rich DNA segment maintaining B-DNA via a unique conformation, (*ii*) the neighboring AT-rich region becomes destabilized and the CG-rich segment is converted to Z-DNA, and finally (*iii*) the B–Z junction is formed by base pairing of the AT-rich region.

Acknowledgements

This work was supported by the National Research Foundation of Korea (NRF) grants [2010-0014199, NRF-C1ABA001-2010-0020480, 2012R1A4A1027750 (BRL)] funded by Korean Government (MEST). This work was also supported by a grant from Next-Generation BioGreen 21 Program (SSAC, no. PJ009041), Rural Development Administration, Korea. We thank the GNU Central Instrument Facility for performing the NMR experiments.

References

[1] A. Herbert, A. Rich, The biology of left-handed Z-DNA, Journal of Biological Chemistry 271 (1996) 11595–11598.
[2] A. Herbert, A. Rich, Left-handed Z-DNA: structure and function, Genetica 106 (1999) 37–47.
[3] T. Schwartz, M.A. Rould, K. Lowenhaupt, A. Herbert, A. Rich, Crystal structure of the Zα domain of the human editing enzyme ADAR1 bound to left-handed Z-DNA, Science 284 (1999) 1841–1845.
[4] T. Schwartz, J. Behlke, K. Lowenhaupt, U. Heinemann, A. Rich, Structure of the DLM-1–Z-DNA complex reveals a conserved family of Z-DNA-binding proteins, Nature Structural Biology 8 (2001) 761–765.
[5] Y.-G. Kim, M. Muralinath, T. Brandt, M. Pearcy, K. Hauns, K. Lowenhaupt, B.L. Jacobs, A. Rich, A role for Z-DNA binding in vaccinia virus pathogenesis, Proceedings of the National Academy of Sciences of the United States of America 100 (2003) 6974–6979.
[6] S.C. Ha, N.K. Lokanath, D. Van Quyen, C.A. Wu, K. Lowenhaupt, A. Rich, Y.G. Kim, K.K. Kim, A poxvirus protein forms a complex with left-handed Z-DNA: crystal structure of a Yatapoxvirus Zα bound to DNA, Proceedings of the National Academy of Sciences of the United States of America 101 (2004) 14367–14372.
[7] S.C. Ha, D. Kim, H.Y. Hwang, A. Rich, Y.-G. Kim, K.K. Kim, The crystal structure of the second Z-DNA binding domain of human DAI (ZBP1) in complex with Z-DNA reveals an unusual binding mode to Z-DNA, Proceedings of the National Academy of Sciences of the United States of America 105 (2008) 20671–20676.
[8] A.G. Herbert, A. Rich, A method to identify and characterize Z-DNA binding proteins using a linear oligodeoxynucleotide, Nucleic Acids Research 21 (1993) 2669–2672.
[9] A. Herbert, J. Alfken, Y.G. Kim, I.S. Mian, K. Nishikura, A. Rich, A Z-DNA binding domain present in the human editing enzyme, double-stranded RNA adenosine deaminase, Proceedings of the National Academy of Sciences of the United States of America 94 (1997) 8421–8426.
[10] A. Herbert, M. Schade, K. Lowenhaupt, J. Alfken, T. Schwartz, L.S. Shlyakhtenko, Y.L. Lyubchenko, A. Rich, The Zα domain from human ADAR1 binds to the Z-DNA conformer of many different sequences, Nucleic Acids Research 26 (1998) 3486–3493.
[11] M. Schade, C.J. Turner, R. Kuhne, P. Schmieder, K. Lowenhaupt, A. Herbert, A. Rich, H. Oschkinat, The solution structure of the Zα domain of the human RNA editing enzyme ADAR1 reveals a prepositioned binding surface for Z-DNA, Proceedings of the National Academy of Sciences of the United States of America 96 (1999) 12465–12470.
[12] Y.-M. Kang, J. Bang, E.-H. Lee, H.-C. Ahn, Y.-J. Seo, K.K. Kim, Y.-G. Kim, B.-S. Choi, J.-H. Lee, NMR spectroscopic elucidation of the B–Z transition of a DNA double helix induced by the Zα domain of human ADAR1, Journal of the American Chemical Society 131 (2009) 11485–11491.
[13] S.C. Ha, K. Lowenhaupt, A. Rich, Y.-G. Kim, K.K. Kim, Crystal structure of a junction between B-DNA and Z-DNA reveals two extruded bases, Nature 437 (2005) 1183–1186.
[14] Y.-M. Lee, H.-E. Kim, C.-J. Park, A.-R. Lee, H.-C. Ahn, S.J. Cho, K.-H. Choi, B.-S. Choi, J.-H. Lee, NMR study on the B–Z junction formation of DNA duplexes induced by Z-DNA binding domain of human ADAR1, Journal of the American Chemical Society 134 (2012) 5276–5283.
[15] F. Delaglio, S. Grzesiek, G.W. Vuister, G. Zhu, J. Pfeifer, A. Bax, NMRPipe: a multidimensional spectral processing system based on UNIX pipes, Journal of Biomolecular NMR 6 (1995) 277–293.
[16] T.D. Goddard, D.G. Kneller, SPARKY 3, University of California, San Francisco, CA, 2003.
[17] J.-H. Lee, A. Pardi, Thermodynamics and kinetics for base-pair opening in the P1 duplex of the *Tetrahymena* group I ribozyme, Nucleic Acids Research 35 (2007) 2965–2974.
[18] M. Gueron, J.L. Leroy, Studies of base pair kinetics by NMR measurement of proton exchange, Methods in Enzymology 261 (1995) 383–413.
[19] J.R. Bothe, K. Lowenhaupt, H.M. Al-Hashimi, Incorporation of CC steps into Z-DNA: interplay between B–Z junction and Z-DNA helical formation, Biochemistry 51 (2012) 6871–6879.